NOTES AND CORRESPONDENCE

The Role of Potential Vorticity Generation in Tropical Cyclone Rainbands

PETER T. MAY AND GREG J. HOLLAND

Bureau of Meteorology Research Centre, Melbourne, Victoria, Australia

19 May 1997 and 16 July 1998

ABSTRACT

The implied heating and potential vorticity generation in tropical cyclone rainbands is derived from observed vertical motion profiles. High levels of potential vorticity generation are found in the stratiform rain regions, sufficient to generate substantial wind maxima along the bands within a couple of hours. Such generation may represent a significant source of potential vorticity for the system as a whole and may have implications for cyclone intensity.

1. Introduction

There has been considerable recent discussion on the role of vortices produced within mesoscale convective systems on the initiation and intensification of tropical cyclones (Ritchie et al. 1993; Harr et al. 1996; Simpson et al. 1997; Ritchie and Holland 1997) and their effect on cyclone tracks (Holland and Lander 1993; Lander and Holland 1993; Ritchie and Holland 1993; Wang and Holland 1995). Less attention has been paid to the potential role played by cyclone rainbands at all stages in the storm life cycle.

Tropical cyclone rainbands are largely made up of extensive regions of stratiform rain with embedded convection showing varied degrees of organization (e.g., Barnes et al. 1991; Ryan et al. 1992; May 1996). Many of these rainbands have midlevel jets (e.g., Willoughby et al. 1984; Jorgensen 1984; Marks 1985; May et al. 1994; Samsury and Zipser 1995), which are associated with distinct local maxima in the radial distribution of vorticity around a cyclone (May et al. 1994). May (1996) suggested that these jets may result from potential vorticity production by the vertical gradient of heating in the stratiform rain regions (Raymond and Jiang 1990). This note is not intended to quantitatively examine the entire potential vorticity budget, but rather explores the potential vorticity production rates associated with this heating gradient and examines some implications for the tropical cyclone as a whole.

The potential positive role of the rainbands in the intensification of storms discussed here is in contrast to the adverse effects often ascribed to them. The bands provide a partial barrier to the low-level inflow limiting the low-level advection of high θ_e air into the storm core (e.g., Barnes et al. 1983; Powell 1990; Samsury and Zipser 1995). Furthermore, the mesoscale descent in the bands below the freezing level will tend to bring low θ_e down from aloft (Samsury and Zipser 1995), thus tending to limit convective activity.

2. Data and method

We utilize satellite, Doppler wind profiler, and radiosonde observations taken during the passage of Tropical Storm Flo in the TCM90 field program (Tropical Cyclone Motion 90, TCM90; Elsberry 1990). These data are described in detail in May et al. (1994). The stratiform rainbands and associated vertical velocity and jet structure are typical of most tropical cyclones. For example, similar data were collected in stratiform rain in rainbands during the passage of Tropical Cyclone Laurence near Darwin (May 1996). However, in that case embedded convection makes the interpretation more difficult.

Raymond and Jiang (1990) estimated the potential vorticity production within stratiform rain areas associated with mesoscale convective systems. The potential vorticity associated with the vertical component of absolute vorticity is defined as

$$q = \rho^{-1}(\zeta_a)\frac{\partial \theta}{\partial z}, \tag{1}$$

where ρ is the air density, ζ_a is the vertical component of the absolute vorticity, θ is potential temperature, and z is the vertical ordinate. Following Raymond and Jiang

Corresponding author address: Dr. Peter T. May, BMRC, GPO Box 1289K, Melbourne, Victoria 3001, Australia.
E-mail: p.may@bom.gov.au

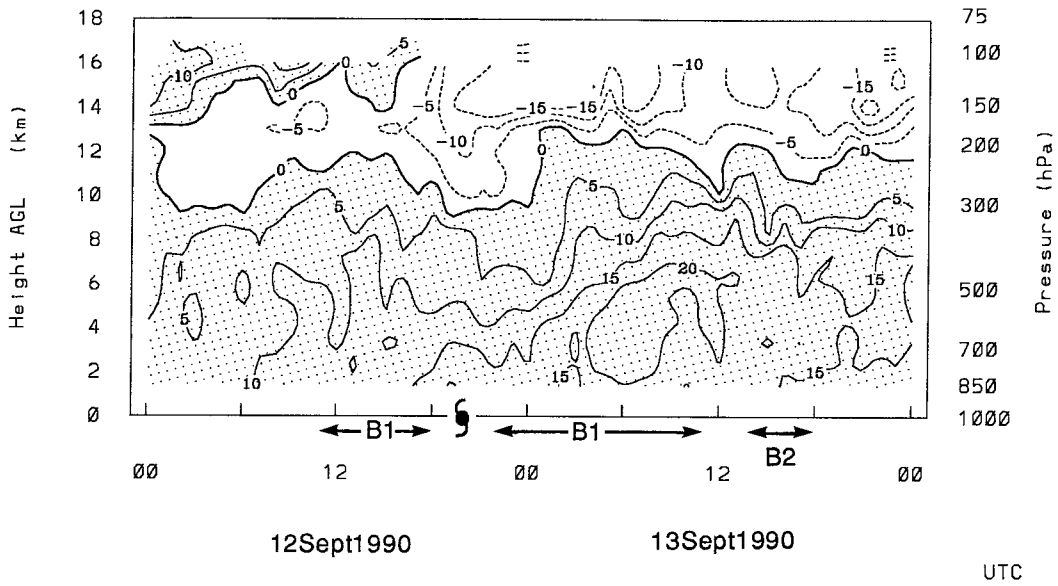

FIG. 1. Tangential wind relative to the center of Tropical Storm Flo as determined from hourly wind measurements with a 50-MHz wind profiler located at Saipan during TCM90 (adapted from May et al. 1994) from 0000 UTC 12 Sep to 0000 UTC 14 Sep 1990. The closest approach of the storm (within the rainband complex) is marked by the cyclone symbol on the time axis, and the period the rainband is overhead is marked as "B1." Here B1 is crossed twice, so that the time–height section is analogous with a spatial section through the rainbands to the north of the storm center.

(1990), the time-rate-of-change of potential vorticity, ignoring horizontal transport, is

$$\frac{dq}{dt} = \rho^{-1}\frac{\partial}{\partial z}(H\zeta_a), \tag{2}$$

where H is the heating rate, which for stable, saturated ascent is simply

$$H = w\left(\frac{\partial\theta_p}{\partial z}\right), \tag{3}$$

where θ_p is the potential temperature of a moist parcel and $\partial\theta_p/\partial z$ is approximately 6 K km^{-1}. The soundings within the rainband are close to saturated up to a height of about 7 km. The results change little using the more realistic heating rate calculation, such as

$$H = \omega\frac{\partial s}{\partial p},$$

where ω is the vertical motion in pressure coordinates and s is the static energy (Yanai et al. 1973), used by May and Rajopadhyaya (1996) for analyzing profiler data. However, for analytic simplicity Eq. (3) is used here.

Combining Eqs. (2) and (3), we have

$$\begin{aligned}\frac{dq}{dt} &\approx \zeta_a\rho^{-1}\left(\frac{\partial w}{\partial z}\right)\frac{\partial\theta_p}{\partial z} + w\left(\frac{\partial}{\partial z}\right)\left(\frac{\partial\theta_p}{\partial z}\right)\\ &\quad + \rho^{-1}w\left(\frac{\partial\zeta_a}{\partial z}\right)\frac{\partial\theta_p}{\partial z}\\ &= \zeta_z\rho^{-1}\left(\frac{\partial w}{\partial z}\right)\frac{\partial\theta_p}{\partial z} + \rho^{-1}w\left(\frac{\partial\zeta_a}{\partial z}\right)\frac{\partial\theta_p}{\partial z},\end{aligned} \tag{4}$$

where the middle term of the top line disappears under the assumption that the $\partial\theta_p/\partial z$ is constant and the latter term is relatively small ($\lesssim$10% of the peak value of the first term). Note that the first term gives an exponential growth in the potential vorticity. As noted above, advection terms have been neglected. While there is certainly significant advection of q along the band, for the purposes of the discussion we assume that the potential vorticity convergence along the band is small compared with the diabatic terms above. The potential impact of advection on the larger circulation will be discussed later. Thus, the direct observations of vertical motion from wind profilers can be used to diagnose potential vorticity generation.

3. Observed vorticity production and its consequences

The tangential wind analysis of Tropical Storm Flo in Fig. 1 contains a distinct jet along the rainband near the freezing level. The storm was moving past the profiler site so the time–height cross section represents an approximate spatial cross section at an oblique angle through the rainbands. Precipitation echoes over the profiler (May et al. 1994) were all indicative of stratiform rain, with vertical velocities of less than 1 m s^{-1} and a distinct brightband signature in the 915-MHz profiler reflectivity. The mean vertical wind profile in the stratiform rainbands (Fig. 2a) contains a distinct mesoscale up–downdraft couplet across the freezing level representing a heating gradient of 4° h^{-1} across the convergence maximum. This couplet arises from a vertical

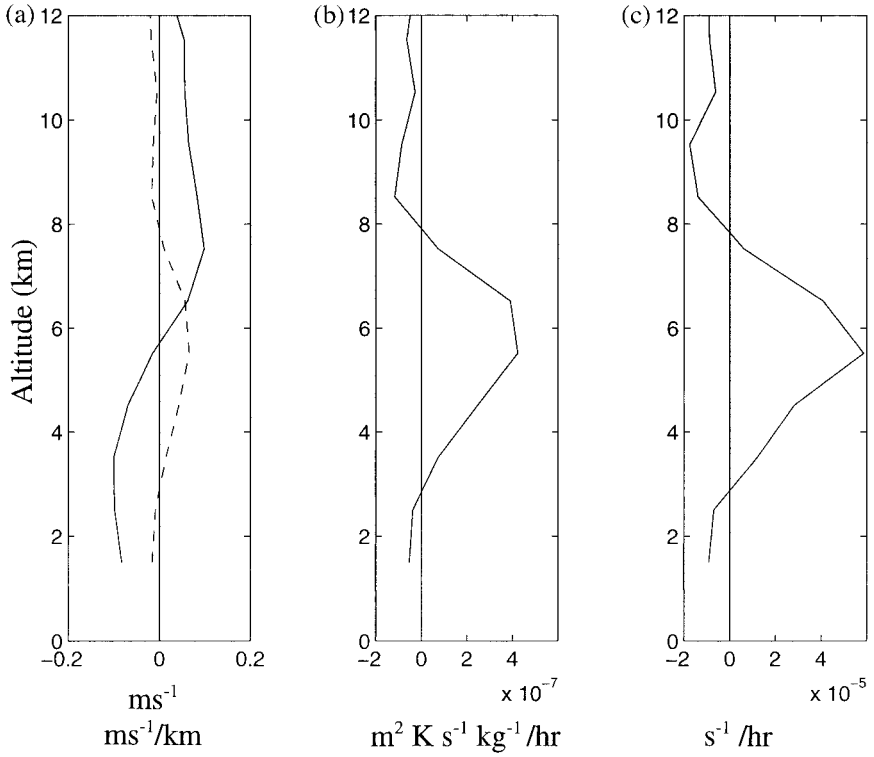

FIG. 2. Profiles of (a) mean vertical wind (solid) and its vertical gradient (dashed), (b) corresponding potential vorticity generation, and (c) vorticity generation assuming that the potential vorticity response is confined to the wind field. See text for details.

heating gradient with evaporational cooling and melting below the stratiform cloud base and condensational heating above.

The resulting potential vorticity production in Fig. 2b is derived from Eq. (4). The dq/dt (b) is estimated using a profile of vorticity that varies as a cosine with height, with a maximum value of $\zeta_a = 2 \times 10^{-4}$ s^{-1} at a height of 5 km and reached a zero value at 13.5 km, similar to the observed vorticity profile in the rainband (Fig. 3). A strong peak in potential vorticity production occurs near the freezing level (~4.6 km). The major factor of the ''peakiness'' of the profile is due to the peak in the heating gradient profile. We can also write

$$\frac{\partial q}{\partial t} = \rho^{-1}\left(\frac{\partial \zeta_a}{\partial t}\right)\frac{\partial \theta}{\partial z} + \zeta_a \frac{\partial}{\partial t}\left(\frac{\partial \theta}{\partial z}\right). \quad (5)$$

A vertical profile of $\zeta_a(\partial/\partial t)(\partial\theta/\partial z)$ averaged over the three radiosonde soundings taken within the rainband has small values (~1/5 the magnitude with noisy time and height structure) compared with $\partial q/\partial t$, except for a thin layer (~200 m thick) close to the freezing level and in the upper levels where advection is probably important (not shown). Since the thermal structure does not change much in the vicinity of the rainbands, this potential vorticity source must be manifested primarily within the wind field so that we can infer the approximate time rate of change of relative vorticity in Fig. 2c. The q production in this approximation essentially reduces to a stretching of the vorticity. This shows that the observed relative vorticity (Fig. 3) in the alongband jet could be generated in about 4 h: a timescale that is small compared with the duration of the rainband and the advection time for a parcel to travel along the band. The approximations used here ignore advection and tilting, but the vorticity production implied is so large that it is an important consideration for storm structure and evolution.

Sustained high rates of production of vorticity in the rainband raise the question of limiting processes, as the vorticity and jet do not continuously increase with time. Observations of the rapid decay of the midlevel jet in Tropical Cyclone Laurence by May (1996) when the stratiform rain region was disrupted also attest to the presence of high levels of dissipation. We suggest that at least three processes may limit the vorticity increase, with each having varying importance, depending on the circumstances and location relative to the cyclone center. These are radial shearing deformation, advection along the band, and vertical flux by moist convection.

The potential vorticity band generated by the diabatic heating in the cloud band will experience substantial shearing deformation increasing toward the cyclone core (e.g., Holland and Dietachmayer 1993), as are the dynamically passive stratiform rain regions. The effect of

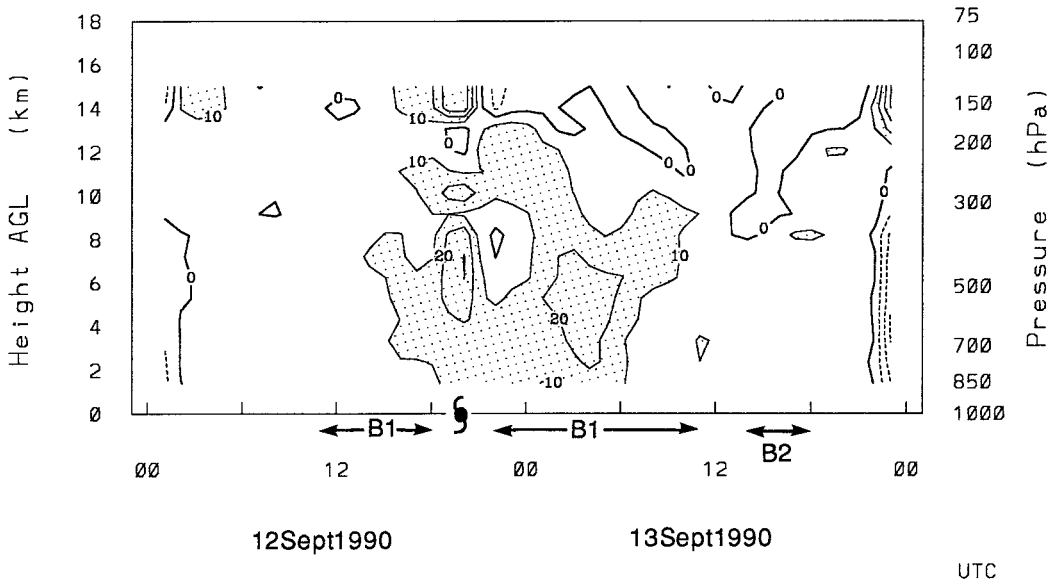

FIG. 3. Analyzed vorticity time–height section determined from hourly wind measurements (adapted from May et al. 1994).

such shearing deformation is to stretch the vorticity into filaments that spiral toward the center of the tropical cyclone (e.g., Ritchie et al. 1993; Holland and Dietachmayer 1993). It is this process that shears the vorticity into the jet profile. The associated jet has higher tangential velocities on the outer side of the vorticity maximum, as occurs in Fig. 1. A logical result of this process is a tight band of potential vorticity wrapped around the core, which can contribute to the symmetric component of vorticity (e.g., Carr and Williams 1989) and thus the cyclone intensity. Also, the vertical velocity data show that the heating dipole responsible for the PV generation is isolated within the band. The shearing, combined with the continued development of vorticity in the rainband sharpens the radial gradient of vorticity/tangential velocity to the point where processes such as the generation of inertia gravity waves may lead to substantial dissipation.

The advecting flow is along the band in a spiral toward the cyclone core. The rainband was about 100 km across, with an embedded 20 m s^{-1} tangential wind maximum. This represents a large momentum flux across the rainband and a period of only about 10 h for the vorticity to be advected into the core region from a radius of about 200 km. This advection time and the expected increased velocities as the air spirals into a region with greater background inertial stability imply that vorticities as high as 10^{-3} s^{-1} are feasible via this mechanism at radii of about 50 km. Furthermore, both the temperature increase with decreasing radius and the pressure decrease act to lower θ surfaces, and in the absence of diabatic forces q will travel on such surfaces. Data from Hawkins and Rubsam (1968) suggest that this descent could be by as much as 2 km, mostly at radii less than 80 km so that vorticity generated between altitudes of 3 and 7 km will descend to near the boundary layer. We speculate that such levels of vorticity generation in the cyclone core region could influence the development of secondary eyewalls and thus indirectly affect the entire intensification cycle of the parent cyclone.

The midlevel vorticity will also be rapidly transferred to the surface in regions where moist convection develops. This disrupts the vorticity development in the stratiform rain regions but could be a source of low-level vorticity for the cyclone core region.

4. Conclusions

We have demonstrated that the midlevel vorticity maximum associated with wind maxima within the rainband of tropical cyclones can be developed by potential vorticity production within the stratiform rain by the mechanisms described by Raymond and Jiang (1990). The rate of production is sufficient to spin up the observed jets in a few hours. Indeed, the implied rate of vorticity generation is comparable to the intensification rate of a typical tropical cyclone. The large areal extent of the rainbands implies that such processes may be a significant potential vorticity source for the cyclone as a whole.

As the radius decreases, larger values of vorticity (and tangential velocity) are expected to develop. This is a testable hypothesis with hurricane reconnaissance data. Furthermore, advection and vorticity increases along the spiral band may affect the cyclone core in a range of ways. One is that downward flux to the surface in moist convection may directly supply vorticity to the low-level

flow. In addition, the substantial concentration of vorticity may play an important role in secondary eyewall generation.

This note has presented a simple calculation of one aspect of the PV budget within tropical cyclone rainbands. The large diagnosed source indicates that more detailed modeling, dual-Doppler airborne radar, and budget studies are warranted to examine the production of potential vorticity within tropical cyclone rainbands, including terms that could not be calculated here, particularly the magnitude and overall contribution of the advective terms.

Acknowledgments. This study forms part of the Australian Tropical Cyclone Coastal Impacts Program. It is partially supported by the Office of Naval research under Grant N-00024-94-1-0493 and by the Australian National Greenhouse Advisory Committee, Department of the Environment, Sport and Territories. Part of this work was performed while P. May was visiting the Cooperative Institute for Research in Environmental Sciences at the University of Colorado supported under NASA Contract NAGW-4146.

REFERENCES

Barnes, G. M., E. J. Zipser, D. Jorgensen, and F. Marks Jr., 1983: Mesoscale and convective structure of a hurricane rainband. *J. Atmos. Sci.,* **40,** 2125–2137.

——, J. F. Gamache, M. A. LeMone, and G. S. Stossmeister, 1991: A convective cell in a hurricane rainband. *Mon. Wea. Rev.*, **119,** 776–794.

Carr, L. E., III, and R. T. Williams, 1989: Barotropic vortex stability to perturbations from axisymmetry. *J. Atmos. Sci.,* **46,** 3177–3191.

Elsberry, R. L., 1990: International experiments to study tropical cyclones in the western North Pacific. *Bull. Amer. Meteor. Soc.*, **71,** 1305–1316.

Harr, P. A., R. L. Elsberry, and J. C. L. Chan, 1996: Transformation of a large monsoon depression to a tropical storm during TCM-93. *Mon. Wea. Rev.*, **124,** 2625–2643.

Hawkins, H. F., and D. T. Rubsam, 1968: Hurricane Hilda, 1964. II. Structure and budgets of the hurricane on October 1, 1964. *Mon. Wea. Rev.,* **96,** 617–636.

Holland, G. J., and G. S. Dietachmayer, 1993: On the interaction of tropical-cyclone-scale vortices. III: Continuous barotropic vortices. *Quart. J. Roy. Meteor. Soc.,* **119,** 1381–1398.

——, and M. Lander, 1993: The meandering nature of tropical cyclone tracks. *J. Atmos. Sci.,* **50,** 1254–1556

Jorgensen, D. P., 1984: Mesoscale and convective-scale characteristics of mature hurricanes. Part I: General observations by research aircraft. *J. Atmos. Sci.,* **41,** 1268–1285.

Lander, M., and G. J. Holland, 1993: On the interaction of tropical-cyclone-scale vortices. I: Observations. *Quart. J. Roy. Meteor. Soc.,* **119,** 1347–1361.

Marks, F. D., 1985: Evolution of the structure of the precipitation in Hurricane Allen (1980). *Mon. Wea. Rev.,* **113,** 907–930.

May, P. T., 1996: The organization of convection in the rainbands of Tropical Cyclone Laurence. *Mon. Wea. Rev.*, **124,** 807–815.

——, and D. K. Rajopadhyaya, 1996: Wind profiler observations of vertical motion and precipitation microphysics of a tropical squall line. *Mon. Wea. Rev.*, **124,** 621–633.

——, G. J. Holland, and W. L. Ecklund, 1994: Wind profiler observations of Tropical Storm Flo at Saipan. *Wea. Forecasting,* **9,** 410–426.

Powell, M. D., 1990: Boundary layer structure and dynamics in outer hurricane rainbands. Part I: Mesoscale rainfall and kinematic structure. *Mon. Wea. Rev.,* **118,** 891–817.

Raymond, D. J., and H. Jiang, 1990: A theory for long-lived mesoscale convective systems. *J. Atmos. Sci.,* **47,** 3067–3077.

Ritchie, E. A., and G. J. Holland, 1993: On the interaction of tropical-cyclone-scale vortices II: Discrete vortex patches. *Quart. J. Roy. Meteor. Soc.,* **119,** 1363–1379.

——, and ——, 1997: Scale interactions during the formation of Typhoon Irving. *Mon. Wea. Rev.,* **125,** 1377–1396.

——, ——, and M. Lander, 1993: Contributions by mesoscale convective systems to movement and formation of tropical cyclones. *Tropical Cyclone Disasters,* J. Lighthill, Z. Zheng, G. J. Holland, and K. Emanuel, Eds., Peking University Press, 286–289.

Ryan, B. F., G. M. Barnes, and E. J. Zipser, 1992: A wide rainband in a developing tropical cyclone. *Mon. Wea. Rev.,* **120,** 431–437.

Samsury, C. E., and E. J. Zipser, 1995: Secondary wind maxima in hurricanes: Airflow and relationship to rainbands. *Mon. Wea. Rev.,* **123,** 3502–3517.

Simpson, J., E. A. Ritchie, G. J. Holland, J. Halverson, and S. Stewart, 1997: Mesoscale interactions in tropical cyclone genesis. *Mon. Wea. Rev*, **125,** 2643–2661.

Wang, Y., and G. J. Holland, 1995: On the interaction of tropical-cyclone-scale vortices. IV: Baroclinic vortices. *Quart. J. Roy. Meteor. Soc.*, **121,** 95–126.

Willoughby, H. E., F. D. Marks, and J. Feinberg, 1984: Stationary and moving convective bands in hurricanes. *J. Atmos. Sci.,* **41,** 3189–3211.

Yanai, M. S., S. Esbenson, and J. H. Chu, 1973: Determination of the bulk properties of tropical cloud clusters from large-scale heat and moisture budgets. *J. Atmos. Sci.,* **30,** 611–627.